Hybrid wood materials with improved fire retardance by bio-inspired mineralisation on the nano- and submicron level

Green Chemistry

COMMUNICATION

View Article Online
View Journal | View Issue

CrossMark click for updates

Cite this: *Green Chem.*, 2015, **17**, 1423

Received 25th September 2014,
Accepted 19th December 2014

DOI: 10.1039/c4gc01862a

www.rsc.org/greenchem

Hybrid wood materials with improved fire retardance by bio-inspired mineralisation on the nano- and submicron level†

Vivian Merk,[a,b] Munish Chanana,*[a,c] Tobias Keplinger,[a,b] Sabyasachi Gaan[d] and Ingo Burgert*[a,b]

Inspired by natural matrix-mediated biomineralisation, we present an artificial calcification approach for wood, which predominately targets the hardly accessible nanoporous cell wall structure rather than the micron-sized void system of the cell lumina. $CaCO_3$ can be deposited with this method deep inside the wood structure. Mineralisation of the wood cell wall architecture with $CaCO_3$ offers a green alternative to conventional fire-retardant systems.

The hierarchical structure of plants provides a utilisable nano- and microstructural skeleton at the cell and cell wall level to develop advanced biocomposites with novel material properties. The wood cell wall consists of stiff paracrystalline cellulose nanofibrils which are oriented in a parallel fashion and are embedded in the amorphous matrix components such as hemicelluloses and lignins.[1,2] This sustainable biocomposite, well known for its excellent mechanical performance,[2] has great potential for wider utilisation, given that a better control of functionalisation processes of the intrinsic hierarchical wood structure is achieved. Although being strong and rigid, the cell wall can be regarded as a compact skeleton since it possesses small nanopores between the cellulose fibrils.

In particular, a hybrid material which consolidates the stiff secondary cell wall of wood with a mineral phase at the nanostructural level can result in a highly desirable material combination.[3–5] A particularly promising but also challenging candidate that could be united with the wood cell wall skeleton to form an advanced and eco-friendly hybrid material for large-scale applications is calcium carbonate ($CaCO_3$).

The insertion of $CaCO_3$ into the wood scaffold is inspired by nature's invention to increase the durability and hardness and reduce the water uptake of the exoskeleton of various species. Screening $CaCO_3$ incidence in nature, it can be noted that it is the most abundant biomineral in corals, pearls, mollusk shells, egg shells and crustacean skeletons,[3–5] whereas calcification occurs rarely in plant cell walls.[6] Generally, plants mineralise their tissues for the end of ion storage and homeostasis in response to unstable calcium levels in the environment.[7,8] $CaCO_3$ is excreted in reef-building coralline algae,[9] wood (vacuoles and cell walls) of oxalogenic trees,[10] specialised idioblast cells in leaves of mulberry trees (*Morus alba*)[11] or as amorphous $CaCO_3$ cystoliths in leaves of certain angiosperms.[8,12] Amorphous calcium carbonate (ACC) has been detected in living organisms either as a transient phase or is stabilised by additional ions, organic macromolecules or proteins.[13–15]

There have been various approaches to chemically modify or functionalise the native cell wall.[16–19] However, its impregnation is highly challenging and only a few studies could prove a relatively cell-wall-specific treatment, in particular with organic or silicon compounds, which resulted in improved material properties.[16–19] A few approaches have been reported, where $CaCO_3$ has been synthesised in wood using aqueous salt solutions,[20] supercritical carbon dioxide[21] or calcium di (methylate) and carbon dioxide.[22] Ionisable surface groups of cellulose[23] and other carbohydrates[24] have been considered as nucleation sites for $CaCO_3$ crystallisation. However, a systematic and eco-friendly modification of the wood cell walls with $CaCO_3$ in aqueous solution at ambient temperature has not been achieved so far. Hence, in this study we investigate a one-pot chemical strategy for the artificial calcification of wood cell walls reminiscent of common biomineralisation pathways in nature.[1,5,25]

In view of practical applications, our aim is to improve one of the major shortcomings of wood, namely the high flamm-

[a]*Wood Materials Science, Institute for Building Materials (IfB), ETH Zürich, Stefano-Franscini-Platz 3, 8093 Zürich, Switzerland.*
E-mail: munish.chanana@uni-bayreuth.de, iburgert@ethz.ch
[b]*Applied Wood Materials Laboratory, EMPA – Swiss Federal Laboratories for Materials Science and Technology, 8600 Dübendorf, Switzerland*
[c]*Physical Chemistry II, University of Bayreuth, University of Bayreuth, Universitätstr. 30, 95447 Bayreuth, Germany*
[d]*Advanced Fibres, EMPA – Swiss Federal Laboratories for Materials Science and Technology, Lerchenfeldstrasse 5, 9014 St. Gallen, Switzerland*

† Electronic supplementary information (ESI) available: Experimental section; IR spectra of $CaCO_3$/wood composites; Raman endmember mappings; PCFC heat release curves; sample mass gain; char yield; equilibrium moisture content; TGA curves; TGA derivatives; semi-quantitative EDX analysis of $CaCO_3$/wood composites, X-ray powder diffraction of mineralised spruce. See DOI: 10.1039/c4gc01862a

ability[26] while retaining its natural attributes such as high porosity and low density. Cellulose pyrolysis (*i.e.* thermal decomposition) accounts for the major heat release in the combustion of wood, involving flaming combustion of volatiles in the gas phase as well as decomposition of char by smoldering or glowing combustion.[21,27] Classical flame-retardant systems (*e.g.* ammonium phosphate-,[28] boron-,[29] silica-,[30] or sulphur-based[31] flame retardants) influence pyrolysis processes chemically by accelerating dehydration and carbonisation, inhibiting the production of flammable volatile gases or fostering the formation of insulating coatings or char layers.[32]

However, many of these fire-retardant formulations present serious environmental and safety hazards due to the release of toxic or carcinogenic compounds during accidental fires, processing, recycling and usage.[33] Halogen-based fire retardants, for instance, release large amounts of corrosive hydrogen halides acting as free radical traps in the flame.[26] In this context, an inert and environmentally benign mineral such as $CaCO_3$ would represent an environmentally friendly and "green" alternative to the classical flame retardants. By incorporating $CaCO_3$ into the wood cell wall structure, the thermal stability is improved by a different mechanism, *i.e.* gases (*e.g.* water, carbon dioxide) released in the endothermic decomposition of hydrated minerals will dilute and cool down the mixture of flammable pyrolysis gases.

Hence, for the artificial calcification of wood, in particular of spruce (a softwood) and beech (a hardwood) we adapted a method originally proposed for the synthesis of ACC microparticles in aqueous solutions.[34–36] This approach consists in the alkaline hydrolysis of dimethyl carbonate precursors in the presence of calcium ions inside the cell wall structure, which is depicted in Fig. 1A. Induced by a pH shift, gaseous carbon dioxide evolves *in situ*,[34] hence concentration gradients across the bulk sample and a rapid mineral precipitation in the wood lumina are circumvented to a great extent. Due to the addition of excess sodium hydroxide solution a quantitative hydrolysis of the precursor dimethyl carbonate can be achieved, throughout the wood samples. In this study, wood samples of 2 cm edge length were completely mineralised (Fig. 1B). In this process, only water-soluble by-products, namely sodium chloride and methanol, are formed, which do not interfere with the nucleation and growth of $CaCO_3$ [35] and can be easily removed by washing and/or drying. In view of process sustainability, common membrane techniques enable the separation of ternary dimethyl carbonate–methanol–water mixtures for the removal of excess unreacted DMC.[37]

As shown in Fig. 1B, the resulting wood/$CaCO_3$ composites and native wood appear very similar macroscopically. Light microscopic images of cross-cut $CaCO_3$/wood composites (Fig. 1C and D) indicated little calcareous minerals filling up the bigger lumina of beech vessels and earlywood tracheids of spruce. These results were confirmed *via* scanning electron microscopy (SEM) of the cross-cut $CaCO_3$/wood composites in the backscattered electron mode (Fig. 2).

In the case of spruce, mineral compounds seem to agglomerate prevailingly along the middle lamellae, primary cell walls and cell corners of vicinal cells where calcium-complexing pectins are abundant.[38–40] Polyuronates offer natural negatively-charged polyelectrolyte calcium-binding sites where $CaCO_3$ nucleation is favoured.[39,40] Electron-rich material (*i.e.* $CaCO_3$) can be observed in the cell walls of beech fibres,

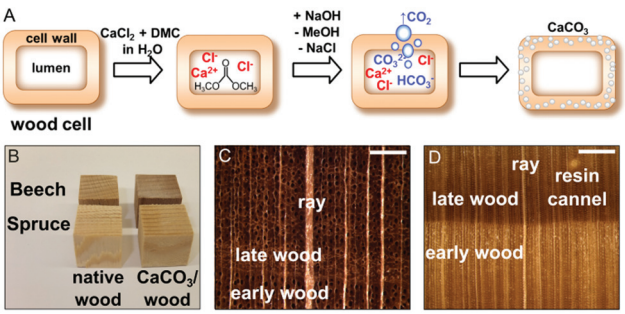

Fig. 1 (A) Schematic depiction of the mineralisation of wood by alkaline hydrolysis of dimethyl carbonate in the presence of calcium ions within the wood matrix. (B) Photo of unmodified and mineralised spruce and beech samples (2 cm edge length). Light microscopic images of mineralised beech (C) and spruce specimens (D). The scale bars in (C) and (D) correspond to 500 μm.

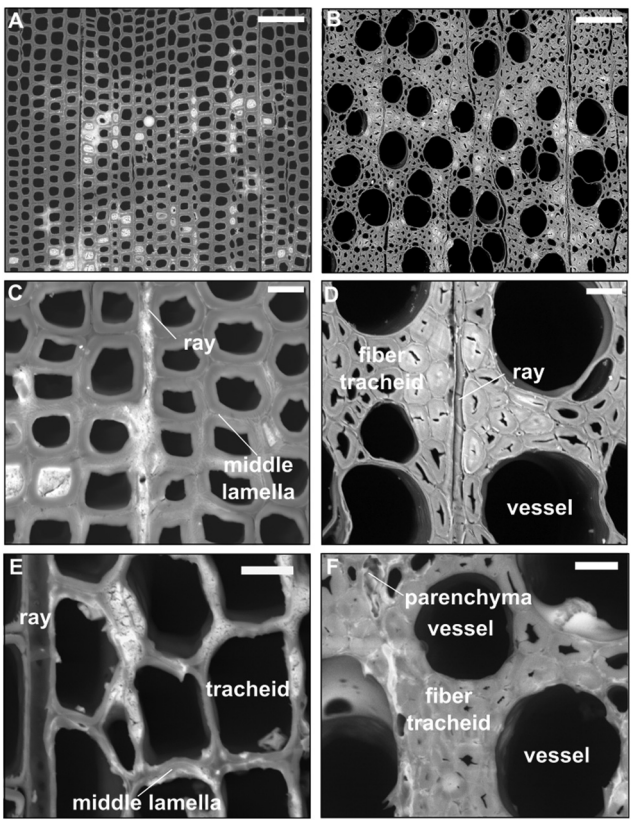

Fig. 2 Low-vacuum scanning electron microscopy of microtome cross-sections of spruce (A, C, E) and beech (B, D, F) $CaCO_3$ composites prepared at [DMC] = [$CaCl_2$] = 1.5 mol L^{-1} prior to drying. SEM images in the backscattered electron mode give evidence of relatively void lumina and depositions of electron-dense material along middle lamellae and rays, within beech fibres and parenchyma cells. Scale-bars correspond to 500 μm (A, B), 100 μm (C, D) and 20 μm (E, F).

within parenchyma cells, as well as spruce latewood tracheids and ray cells (Fig. 2A, B, D and E respectively) at higher magnifications. Judging from the morphological features, the electron-lucent deposits appear amorphous, although further analytical characterisation of the minerals refers to dried samples due to the necessary sample preparation.

Furthermore, the mineral distribution in the wood bulk was investigated *via* SEM/EDX. The semi-quantitative energy-dispersive X-ray point microanalysis of the CaK_α line brings a further proof of the presence of calcium-containing mineral incorporated into the wood cell walls of both species, sodium chloride as a side product of the process and unreacted calcium chloride (Fig. S12–17†). Hence, the predominant mineral deposition takes place in the nano- and submicron-sized pores of the wood cell wall structure. A plausible explanation for this could be the interplay of capillary forces and the evolution of gaseous CO_2. Due to the capillary forces, the liquid phase with the dissolved precursors is imbibed into the nano- and submicron pores, whereas due to the evolution of CO_2 bubbles, which presumably will gather and grow in the bigger cell voids (*i.e.* cell lumina and vessels), the mineral precipitation in these large pores of wood is hindered. Furthermore, EDX suggests a non-quantitative reaction of $CaCl_2$ and DMC to $CaCO_3$ due to the highly saturated precursor solutions employed in this study. Nonetheless, the highly water-soluble salts NaCl and $CaCl_2$ can be removed by washing in slightly basic water, as verified by XRD (Fig. S16 and 17, ESI†). For an industrial application as a flame-retardant, sodium chloride in addition to $CaCO_3$ is beneficial due to the higher overall mineral content and increased wood humidity (Fig. 7, ESI†).

$CaCO_3$ has been detected in bulk wood by infrared spectroscopy (Fig. S1, ESI†) and X-ray powder diffraction (S18, ESI†), but these techniques do not provide insight into the spatial distribution of $CaCO_3$ over the wood cell hierarchy. Using confocal Raman microscopy we investigated the mineralogy and localisation of $CaCO_3$ within the wood tissue in greater detail. The most prominent CO_3^{2-} vibration absorption (ν_1) of $CaCO_3$ polymorphs lies in the spectral range of 1089–1069 cm^{-1} [41,42] partly overlapping with the cellulose bands of wood in the wavenumber area 1090–1105 cm^{-1}.[43] Spectral features allow to discriminate among the possible crystalline $CaCO_3$ polymorphs,[41] amorphous and hydrated forms.[42,44] This is why small and evenly distributed amounts of $CaCO_3$ can hardly be detected by mere peak integration. However, vertex component analysis[45,46] allows for deconvoluting the hyperspectral dataset. This multivariate method furnishes representative endmember spectra for the most distinct cell wall components, namely aromatic lignin, carbohydrates, water or $CaCO_3$. Colour-coded mappings (Fig. 3) reflect the cell wall composition by visualising the similarity between each

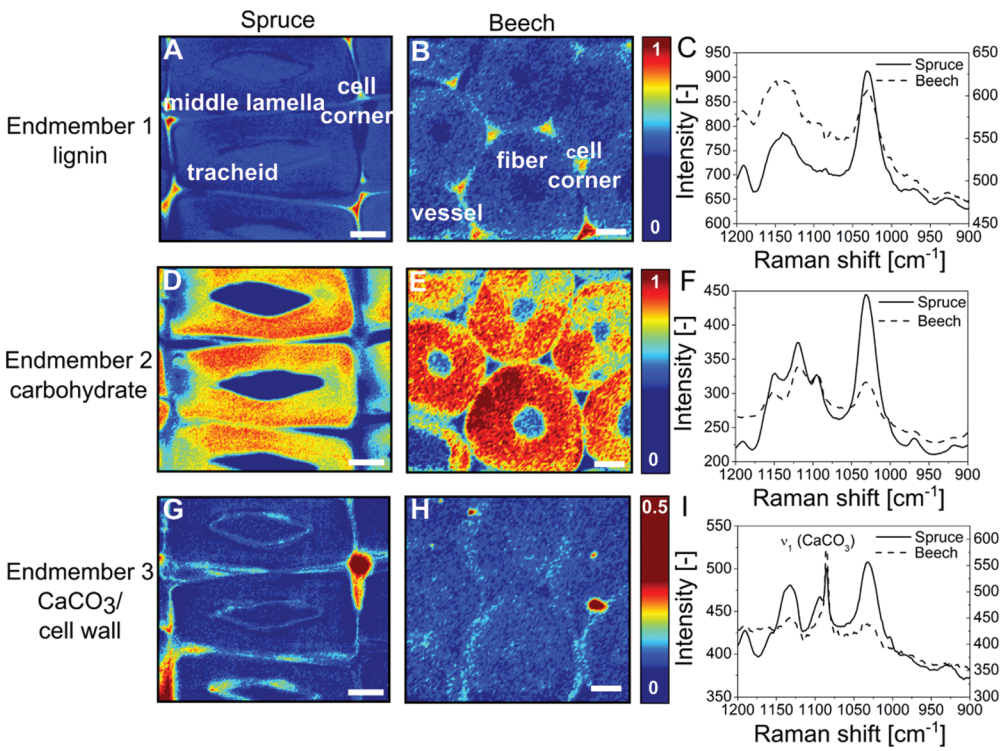

Fig. 3 Raman mappings of $CaCO_3$/wood composites prepared at [DMC] = [$CaCl_2$] = 1.0 mol L^{-1} according to VCA analysis showing endmembers of spruce (A, D, G, solid line) and beech (B, E, H, dashed line) in the range |1200–900 cm^{-1}|. Endmember 1 (A, B): lignin-rich cell corners and middle lamellae (1125–1175 cm^{-1}). Endmember 2 (D, E): secondary cell wall carbohydrates (1112 cm^{-1}, 1154 cm^{-1}). Endmember 3 (G, H): $CaCO_3$ mineral (1080–1090 cm^{-1}) prevailingly in middle lamella and cell corners. (C, F, I): endmember spectra for spruce (solid line) and beech (dashed line) in the range |1200–900 cm^{-1}|. The left axes in 3C and 3I refer to spruce, the right axis to beech. Scale-bars in A, D, G correspond to 10 μm and in B, E, H to 5 μm, respectively.

collected spectrum and the respective endmember spectrum (Fig. 3C, F and I). An endmember with an absorption band at 1140–1160 cm^{-1} can be attributed to the aromatic polymer lignin (Fig. 3A and B) which is most abundant in cell corners and middle lamella at the boundary between vicinal cells. Endmembers with peaks at 1095 cm^{-1}, 1118 cm^{-1} and 1151 cm^{-1} represent secondary (Fig. 3D–F) (S2) cell walls (Fig. S2d–f, ESI†). The S1 cell wall can be discerned by a higher height of the orientation-sensitive cellulose peak at 1095 cm^{-1}. In Fig. 3G and H, the strong ν_1 ($CaCO_3$) vibration at 1086 cm^{-1} together with cell-wall-sensitive spectral bands indicates the presence of calcite within spruce tracheids (Fig. 3A, D and G) and beech fibres (Fig. 3B, E and H) predominantly at the boundary between interconnected cells.

To evaluate the material improvement based on the nanoscale modification, the macroscopic characteristics of the hybrid material are of particular relevance. For instance, hierarchically structured crystalline and amorphous $CaCO_3$ minerals give rise to the superior mechanical properties of chitineous lobster skeletons.[47] Using the mild modification approach of controlled DMC hydrolysis Vilela *et al.* reported a higher mechanical performance of $CaCO_3$/cellulose nanocomposite materials compared to native cellulose.[48] In this work we have investigated the fire behaviour of the inorganic/wood composites (in micro-scale) using pyrolysis combustion flow calorimetry (PCFC) and thermogravimetric analysis. It is evident that mineralised spruce (Fig. 4A) remains physically more intact than untreated spruce after a prolonged heat treatment in a muffle furnace (20 min, 250 °C). The complex line shape of the heat release rate curves of PCFC reflects the successive pyrolysis of the wood constituents hemicellulose, cellulose and lignin, as illustrated in Fig. 4B for beech, was deconvoluted by using a multiple Gaussian fitting technique.

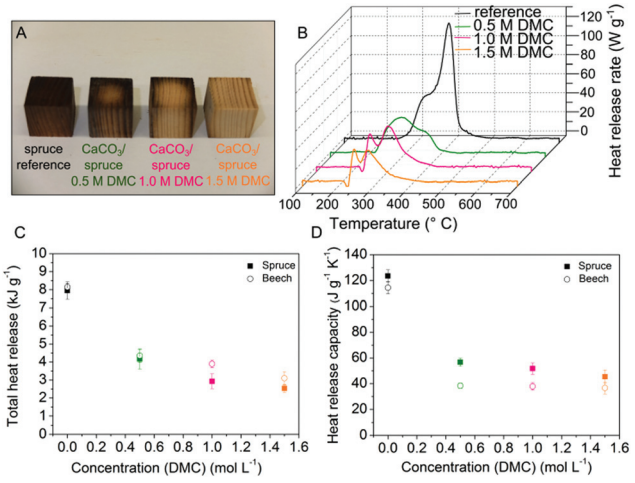

Fig. 4 (A) Photo of native spruce and spruce/$CaCO_3$ composites after heat treatment in a muffle furnace (20 min, 250 °C). (B) Typical temperature-dependent heat release rate curves from pyrolysis combustion flow calorimetry (PCFC) of beech samples after base-line correction. The key parameters total heat release (C) and heat release capacity (D) of spruce and beech are plotted as a function of the precursor concentration [DMC] = [$CaCl_2$].

HRR curves of spruce timber presented in Fig. S4 (ESI†) show one dominant heat release rate maximum originating from the exothermic oxidation of aliphatic cellulose units at 350 °C[27,32] overlapped by a high-temperature shoulder from lignin degradation present in all measured HRR spectra.[49,50] Beech decomposes by a two-step (second order) process through thermal degradation of hemicelluloses at 270 °C followed by cellulose pyrolysis around 350 °C.[49] The incorporation of minerals into the wood architecture affects the cellulose thermal decomposition by reducing the formation of volatiles. The fire properties, namely the total heat of combustion, the heat release capacity and the char residue are significantly improved (Fig. 4C and D, Fig. S6†).

The net heat of combustion of the $CaCO_3$/wood composites measured by pyrolysis combustion flow calorimetry decreased to approximately a third (32–38%) compared to unmodified wood (Fig. 4C). A crucial indicator of fire hazard is the tendency to ignite objects nearby or to maintain flaming combustion. Thus, the potential for fire propagation is mainly assessed by the heat release capacity.[51] Compared to native wood the heat release capacity of the $CaCO_3$/wood composites was found to decrease substantially to 37% of the original value for spruce and 32% for beech (Fig. 4D). Notably, total heat release and heat release capacity values obtained for spruce/$CaCO_3$ composites ([DMC] = 1.5 mol L^{-1}) resemble those reported for halogenated high-performance polymers like poly(tetrafluoroethylene), Teflon™ (THR = 3.7 kJ g^{-1}, HRC = 35 J g^{-1} K^{-1} (ref. 52)) commonly used as heat-resistant coatings. Since the char yield of the composites is approximately doubled compared to native wood (Fig. S6†) the embedded mineral possibly contributes to the fire-retardant capacity of wood.

Furthermore, the incorporated $CaCO_3$ also improves the thermal stability of wood materials. The equilibrium moisture content of the mineralised samples increased as a function of the DMC content (Fig. S7†), likely due to residual sodium chloride in the wood composite, as detected by SEM-EDX (Fig. S12–17†) and XRD (Fig. S18†). Hence, gases (*e.g.* water vapour, carbon dioxide) released in the endothermic decomposition of hydrated minerals may have a diluting and cooling effect on the flammable pyrolysis gases. Furthermore, the inorganic matrix diluents also improve the fire performance by fostering the self-insulating char formation of wood and inhibiting heat transfer and smoke evolution.[53,54] $CaCO_3$, as a weak base, might catalyse the pyrolytic decomposition/depolymerisation of cellulose favouring the production of stable char and non-flammable gases over levoglucosan and other tar anhydrosugars.[55–57] Additionally, TGA data confirm a lowered decomposition temperature and an increased char formation (Fig. S8–11†) for the treated wood samples.

Conclusions

In conclusion, the insertion of $CaCO_3$ into the wood scaffold is inspired by nature's invention to increase the durability and

hardness and reduce the water uptake of the exoskeleton of various species. More importantly, it transfers the principle to a technical level by addressing a severe timber engineering problem. The bio-inspired mineralisation as proposed in the current work highly improves the flame retardancy of wood and hence, considerably expands its reliability in construction without impairing the intrinsic key benefits of wood arising from its biological nature. The fact that a softwood (spruce) and a hardwood (beech) gave similar results under similar treatment conditions, shows the versatility of the process. We conclude that the specific material combination of wood and $CaCO_3$ results in a hybrid material that has the potential to become one of the key construction materials, because of its improved reliability on top of a renewable nature, positive carbon footprint, eco-friendliness, and excellent mechanical performance in view of a still comparably low density. Above all, the concept of wood–mineral nanocomposites making use of a directed mineralisation in the hierarchical scaffold of the wood material opens new ways to develop a multitude of advanced hybrid-materials, based on various mineral combinations and a vast diversity of wood species.

Acknowledgements

We thank the Bundesamt für Umwelt (BAFU) and Lignum, Switzerland for the financial support of the Wood Materials Science group. The authors declare no competing financial interest.

Notes and references

1 P. Fratzl and R. Weinkamer, *Prog. Mater. Sci.*, 2007, **52**, 1263–1334.
2 L. Salmen and A. M. Olsson, *J. Pulp Pap. Sci.*, 1998, **24**, 99–103.
3 F. C. Meldrum, *Int. Mater. Rev.*, 2003, **48**, 187–224.
4 S. Weiner and L. Addadi, *J. Mater. Chem.*, 1997, **7**, 689–702.
5 S. Weiner and L. Addadi, in *Annual Review of Materials Research*, ed. D. R. Clarke and P. Fratzl, 2011, vol. 41, pp. 21–40.
6 H. J. Arnott and F. G. E. Pautard, Calcification in plants, in *Biological Calcification: Cellular and molecular aspects*, ed. H. Schraer, Appleton-Century-Crofts, Educational Division, Meredith Corporation, New York, 1970, pp. 375–446.
7 M. A. Webb, *Plant Cell*, 1999, **11**, 751–761.
8 M. G. Taylor, K. Simkiss, G. N. Greaves, M. Okazaki and S. Mann, *Proc. R. Soc. London, B*, 1993, **252**, 75–80.
9 T. F. Goreau, *Ann. N. Y. Acad. Sci.*, 1963, **109**, 127–167.
10 G. Cailleau, O. Braissant and E. P. Verrecchia, *Biogeosciences*, 2011, **8**, 1755–1767.
11 I. Nitta, A. Kida, Y. Fujibayashi, H. Katayama and Y. Sugimura, *Protoplasma*, 2006, **228**, 201–208.
12 A. Gal, V. Brumfeld, S. Weiner, L. Addadi and D. Oron, *Adv. Mater.*, 2012, **24**, OP77–OP83.
13 L. Addadi, S. Raz and S. Weiner, *Adv. Mater.*, 2003, **15**, 959–970.
14 A. Gal, S. Weiner and L. Addadi, *J. Am. Chem. Soc.*, 2010, **132**, 13208–13211.
15 J. Aizenberg, L. Addadi, S. Weiner and G. Lambert, *Adv. Mater.*, 1996, **8**, 222–226.
16 S. Kumar, *Wood Fiber Sci.*, 1994, **26**, 270–280.
17 E. Cabane, T. Keplinger, V. Merk, P. Hass and I. Burgert, *ChemSusChem*, 2014, **7**, 1020–1025.
18 M. A. Ermeydan, E. Cabane, P. Hass, J. Koetz and I. Burgert, *Green Chem.*, 2014, **16**, 3313–3321.
19 C. Mai and H. Militz, *Wood Sci. Technol.*, 2004, **37**, 339–348.
20 C. Y. Wang, C. Y. Liu and J. Li, in *Environment Materials and Environment Management Pts 1–3*, ed. Z. Y. Du and X. B. Sun, Trans Tech Publications Ltd, Stafa-Zurich, 2010, pp. 1712–1715.
21 C. Tsioptsias and C. Panayiotou, *J. Mater. Sci.*, 2011, **46**, 5406–5411.
22 S. Klaithong, D. Van Opdenbosch, C. Zollfrank and J. Plank, *Z. Naturforsch., B: Chem. Sci.*, 2013, **68**, 533–538.
23 H. Matahwa, V. Ramiah and R. D. Sanderson, *J. Cryst. Growth*, 2008, **310**, 4561–4569.
24 A. Rao, J. K. Berg, M. Kellermeier and D. Gebauer, Sweet on Biomineralization: Effects of Carbohydrates on the Early Stages of Calcium Carbonate Crystallization, *Eur. J. Mineral.*, 2014, **26**, 537.
25 J. W. Morse, R. S. Arvidson and A. Lüttge, *Chem. Rev.*, 2007, **107**, 342–381.
26 R. M. Rowell, *Handbook of Wood Chemistry and Wood Composites*, CRC Press, Boca Raton, 2012.
27 Y. Sekiguchi and F. Shafizadeh, *J. Appl. Polym. Sci.*, 1984, **29**, 1267–1286.
28 M. Hagen, J. Hereid, M. A. Delichatsios, J. Zhang and D. Bakirtzis, *Fire Saf. J.*, 2009, **44**, 1053–1066.
29 G. Tondi, L. Haurie, S. Wieland, A. Petutschnigg, A. Lacasta and J. Monton, *Fire Mater.*, 2013, n/a–n/a.
30 I. Simkovic, H. Martonova, D. Manikova and O. Grexa, *J. Appl. Polym. Sci.*, 2005, **97**, 1948–1952.
31 I. Simkovic, H. Martvonova, D. Manikova and O. Grexa, *Fire Mater.*, 2007, **31**, 137–145.
32 T. Hirata, S. Kawamoto and T. Nishimoto, *Fire Mater.*, 1991, **15**, 27–36.
33 A. R. Horrocks, *Fire retardant materials*, CRC Press, Boca Raton, Fla., 2001.
34 M. Faatz, F. Gröhn and G. Wegner, *Adv. Mater.*, 2004, **16**, 996–1000.
35 M. Faatz, F. Gröhn and G. Wegner, *Mater. Sci. Eng., C*, 2005, **25**, 153–159.
36 K. Gorna, M. Hund, M. Vučak, F. Gröhn and G. Wegner, *Mater. Sci. Eng., A*, 2008, **477**, 217–225.
37 W. Won, X. Feng and D. Lawless, *J. Membr. Sci.*, 2002, **209**, 493–508.
38 K. H. Caffall and D. Mohnen, *Carbohydr. Res.*, 2009, **344**, 1879–1900.
39 G. T. Grant, E. R. Morris, D. A. Rees, P. J. C. Smith and D. Thom, *FEBS Lett.*, 1973, **32**, 195–198.

40 M. C. Jarvis, *Plant, Cell Environ.*, 1984, **7**, 153–164.
41 C. G. Kontoyannis and N. V. Vagenas, *Analyst*, 2000, **125**, 251–255.
42 M. M. Tlili, M. B. Amor, C. Gabrielli, S. Joiret, G. Maurin and P. Rousseau, *J. Raman Spectrosc.*, 2002, **33**, 10–16.
43 N. Gierlinger and M. Schwanninger, *Plant Physiol.*, 2006, **140**, 1246–1254.
44 L. Brecevic and A. E. Nielsen, *J. Cryst. Growth*, 1989, **98**, 504–510.
45 J. M. Nascimento and J. M. Bioucas Dias, *IEEE Trans. Geosci. Remote Sens.*, 2005, **43**, 898–910.
46 N. Gierlinger, *Front. Plant Sci.*, 2014, 5.
47 H. O. Fabritius, C. Sachs, P. R. Triguero and D. Roobe, *Adv. Mater.*, 2009, **21**, 391–400.
48 C. Vilela, C. S. R. Freire, P. A. A. P. Marques, T. Trindade, C. Pascoal Neto and P. Fardim, *Carbohydr. Polym.*, 2010, **79**, 1150–1156.
49 F. Yao, Q. Wu, Y. Lei, W. Guo and Y. Xu, *Polym. Degrad. Stab.*, 2008, **93**, 90–98.
50 M. Brebu and C. Vasile, *Cellul. Chem. Technol.*, 2010, **44**, 353–363.
51 R. E. Lyon and R. N. Walters, *J. Anal. Appl. Pyrolysis*, 2004, **71**, 27–46.
52 R. N. Walters and R. E. Lyon, *J. Appl. Polym. Sci.*, 2003, **87**, 548–563.
53 P. Hornsby, in *Fire Retardancy of Polymeric Materials*, CRC Press, 2nd edn, 2009, pp. 163–185.
54 T. R. Hull, A. Witkowski and L. Hollingbery, *Polym. Degrad. Stab.*, 2011, **96**, 1462–1469.
55 F. Shafizadeh, *J. Anal. Appl. Pyrolysis*, 1982, **3**, 283–305.
56 C. Di Blasi, A. Galgano and C. Branca, *Ind. Eng. Chem. Res.*, 2009, **48**, 3359–3369.
57 D. J. Nowakowski and J. M. Jones, *J. Anal. Appl. Pyrolysis*, 2008, **83**, 12–25.